

# Preparation and Characterization of Poly(methyl methacrylate)–Clay Nanocomposites via Melt Intercalation: The Effect of Organoclay on the Structure and Thermal Properties

Sandeep Kumar,<sup>1</sup> Jyoti P. Jog,<sup>2</sup> Upendra Natarajan<sup>1</sup>

<sup>1</sup>Division of Polymer Chemistry, National Chemical Laboratory, Pune 411008, India

<sup>2</sup>Division of Chemical Engineering, National Chemical Laboratory, Pune 411008, India

Received 30 December 2001; accepted 9 September 2002

**ABSTRACT:** Nanocomposites of poly(methyl methacrylate) (PMMA) with layered silicates were prepared by the melt mixing route. The PMMA–montmorillonite hybrids were characterized by wide-angle X-ray diffraction, thermogravimetric analysis (TGA), and differential scanning calorimetry (DSC). Except for the hybrid formed with unmodified sodium montmorillonite, where a change in distribution of clay platelet stacks was observed without polymer intercalation, the use of organically modified montmorillonites produced well-intercalated systems. An increase in the separation of the clay layers due to polymer intercalation was observed in the range 7–14 Å. TGA thermographs indicated that the onset of decomposition increased by 15–30°C, de-

pending on the organoclay, as compared to PMMA itself. DSC results showed the existence of a glass-transition temperature ( $T_g$ ) for all the hybrids and also showed that the  $T_g$  of the hybrids were lower (by ~10%) compared to that of PMMA. Among the various modifiers, the ones that were relatively more polar favored a greater extent of intercalation of PMMA into the clay layers. The thermal stabilities of the nanocomposites were superior to that of PMMA and were controlled by the stability of the organoclay and its interaction with PMMA. © 2003 Wiley Periodicals, Inc. *J Appl Polym Sci* 89: 1186–1194, 2003

**Key words:** nanocomposites; structure; thermal properties

## INTRODUCTION

Clay-based polymer nanocomposites are an attractive set of hybrid materials, from a technological perspective, providing avenues for interesting and useful investigation of complex confined systems.<sup>1–4</sup> Clays, as layered silicates, present themselves as an interesting species of fillers to be used in current industrial research. Polymer-layered silicate nanocomposites have gained importance in recent years because of their superior thermal, mechanical, and gas-barrier properties as compared to the polymer itself. The enhancement of these properties occurs with nanoscale heterogeneity and dispersion of only a few percentage points of either pristine or organically modified silicates dispersed in the polymer matrix. These performance improvements largely depend on the spatial distribution, the arrangements of intercalating polymer chains, and the interfacial interaction between the silicate layers and the polymer. Natural montmorillonite (2:1 aluminosilicate) (MMT) carries a distribution of negative charges in its inorganic framework so that the framework interacts electrostatically with

metal cations present or occurring in its interlayer gallery. Pristine montmorillonite is generally incompatible with hydrophobic polymers because of its hydrophilic nature. However, it is compatible with hydrophilic or polar polymers, for example, poly(ethylene oxide) (PEO) and poly(vinyl pyrrolidone) (PVP) among several others. This compatibility between the clay and polymer facilitates the intercalation of the polymer into the interlayer space between the successively stacked silicate layers.

The enhancement of favorable interactions between montmorillonite and hydrophobic polymers can be brought about by the organic modification of montmorillonite via the replacement of the interlayer metal cations by various organic cations, such as alkylammonium cations.<sup>1,3,4</sup> Most of the organoclays that are used for nanocomposite investigations contain quaternary ammonium ions as the organic modifiers, with the list being too exhaustive to be laid down here. Such an organic modification provides two benefits. First, the interlayer space between the layered silicates increases as a result of the long-chain alkylammonium cations, thereby relatively weakening the interactions between the successive clay layers. Second, these small molecules electrostatically bonded to silicates render montmorillonite more molecularly compatible with the polymer molecules. Polymer–clay nanocom-

Correspondence to: U. Natarajan (upendra@poly.ncl.res.in).

posites show unusual properties that are not shown by conventional composites, primarily thought to be because of confinement effects and because of large interfacial areas per unit volume of the layered silicates.

Nonreactive melt processing of a polymer with clays is an effective approach to the preparation of thermodynamically compatible nanocomposites. The technique involves the annealing, statically or under shear, of a mixture of polymer and the inorganic host above the glass-transition temperature ( $T_g$ ) of the polymer. The driving force for the intercalation can be rationalized based on three competing effects, namely, (1) the decrease in conformational entropy of the flexible polymer chains when confined between the silicate layers, (2) an increase in the conformational entropy of the organic modifiers as layers to accommodate the polymer, and (3) a net energy gain associated with the establishment of more favorable secondary interactions between the polymer and the organically modified layered silicate (OLS) than originally present in the unintercalated OLS.

Poly(methyl methacrylate) (PMMA) is an optically transparent material with technological importance because of its high surface resistivity, high weatherability, and light resistance. PMMA nanocomposites offer the potential for reduced gas permeability and improved thermal and mechanical properties without any loss of optical clarity. Most of the reports on PMMA-clay nanocomposites have been based on *in situ* polymerization routes for their preparation,<sup>5-10</sup> mainly emulsion polymerization and solution polymerization methods. The first account of the synthesis of PMMA-clay nanocomposites was given by Blumstein,<sup>5</sup> where natural sodium montmorillonite ( $\text{Na}^+\text{MT}$ ) was used along with methyl methacrylate (MMA) via free-radical polymerization in the presence of the clay. Biasci et al.<sup>6</sup> obtained intercalated PMMA-clay nanocomposites by two methods: (1) the polymerization of MMA with montmorillonite modified by 2-(*N*-methyl-*N,N*-diethylammonium iodide) ethyl acrylate and (2) the direct intercalation of MMA polymers with an OLS. Lee and Jang<sup>7</sup> prepared PMMA-clay hybrids by emulsion polymerization techniques, and they got intercalated structures. Huang and Brittain<sup>10</sup> prepared PMMA-clay hybrids by the suspension polymerization technique, and they got partially exfoliated structures. The observed feature common to all these studies was the increase in the  $T_g$  of the PMMA-clay hybrids on the formation of the nanocomposites relative to the  $T_g$  of PMMA itself. However, interestingly, a decrease in the  $T_g$  by hybrid formation has been observed in extruded samples prepared by the melt mixing route, although the underlying mechanism for this behavior is not clear at this time.<sup>11,12</sup> Another study on PMMA-clay nanocomposites prepared by the melt mixing route has been

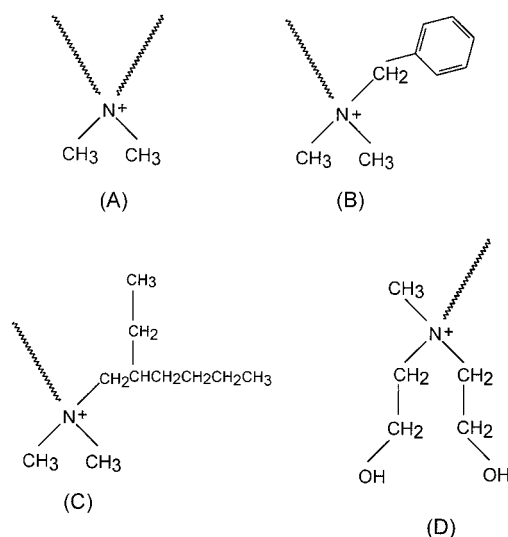


**Figure 1** Chemical structures of the quaternary ammonium modifiers: (A) 2M2HT, (B) 2MBHT, (C) 2MHTL8, and (D) MT2EtOH.

recently reported, where up to 1 wt % of an organoclay (trade name Clayton APA, Southern Clay Products, Inc.) was used; however, no results on the behavior of  $T_g$  or the degradation behavior were reported.<sup>13</sup>

In this work, we present for the first time a study on the effects of the nature of organically modified montmorillonite on the nanocomposites that are formed with PMMA via the melt mixing route. The motivation for such a study stemmed from the lack of sufficient understanding and interest the use of new organoclay systems for PMMA hybrids formed by interactions with a variety of structurally different organoclays. PMMA interestingly shows interactions with montmorillonite, and therefore, extensive studies can pave the way for a more comprehensive understanding of intercalated polymer systems. The results presented here include wide-angle X-ray diffraction (WAXD) patterns of the hybrid structures, direct observation of the nanoscale structure via transmission electron microscopy (TEM), and the thermal properties ( $T_g$ 's and the onset of thermal degradation and weight loss curves) of these hybrids.

## EXPERIMENTAL

### Materials and methods

Sodium montmorillonite ( $\text{NaMT}$ ) and various other organically modified montmorillonites used in this study were supplied by Southern Clay Products, Inc. (Gonzales, TX). The structures of the modifiers are shown in Figure 1. The clays used for our study were Cloisite  $\text{Na}^+\text{MT}$  [cation exchange capacity (CEC) = 90 meq/100 g], Cloisite10A [with the organic modifier dimethyl-benzyl-hydrogenated tallow ammonium (2MBHT); CEC = 125 meq/100 g], Cloisite20A [with

the organic modifier dimethyl-dihydrogenated tallow ammonium (2M2HT); CEC = 95 meq/100 g], Cloisite25A [with the organic modifier dimethyl-hydrogenated tallow 2-ethylhexyl ammonium (2MHTL8); CEC = 95 meq/100 g], and Cloisite30B [with the organic modifier methyl tallow bis-2-hydroxyethyl ammonium (MT2EtOH); CEC = 90 meq/100 g]. The average particle size (80 vol %) of the clays used varied in the range 2–13  $\mu$ . The virgin PMMA (Acrypol-p 8015) was provided by the Polymer Corporation of Gujarat Ltd. had a melt flow index of 1.5 g/min, and was used without further modification. PMMA and all the clays used for the experiments were dried at 65°C in a vacuum oven for 12 h before mixing. PMMA and the required amounts of various clays (10 wt % in each hybrid) were dry-mixed and melt-blended at a temperature of 175°C in a Brabender plasticorder mixer at two speeds, 30 and 60 rpm, for 30 min.

### Characterization

Characterization of the prepared samples was performed at speeds of 30 and 60 rpm. The difference in the results was not appreciable; therefore, only the analyses for the samples prepared with 30 rpm are presented in the later sections. WAXD patterns were recorded on a Rigaku (Japan) diffractometer with Cu K $\alpha$  radiation at 50 kV and 120 mA. The experiments were performed in a scan range of  $2\theta = 2$ –15° with a scan speed of 1°/min on compression-molded samples. The thermal properties of the composites were measured by differential scanning calorimetry (DSC) and thermogravimetric analysis (TGA). A Mettler DSC Fp 85 was used for the measurements in the temperature range 50–230°C, a range that was sufficient and encompassed as well as went well above the  $T_g$  of PMMA. Typically, a sample of about 10 mg was heated first from 50 to 260°C at a heating rate of 10°C/min to relieve any thermal history of the glassy state. Then, the sample was allowed to cool to 50°C

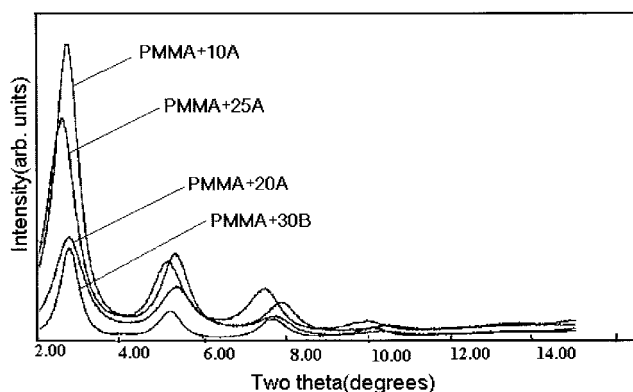


**Figure 2** Combined WAXD patterns of nanocomposites made from PMMA and various organoclays.

and was subsequently reheated from 50 to 160°C. Heating was repeated at the same rate. The data obtained from the second scan was used for the  $T_g$  determination of the polymer and the hybrids. TGA measurements were carried out on a PerkinElmer TGA-7. Samples of about 4 mg were heated from 50 to 650°C at a heating speed of 10°C/min under a nitrogen atmosphere. The same heating rates were used for PMMA and the hybrid samples. The experiments were repeated on some samples to ensure the accuracy of the results.

## RESULTS AND DISCUSSION

### X-ray diffraction and nanocomposite structure

The WAXD results are shown in Figure 2 for all four hybrids (PMMA–Cloisite10A, PMMA–Cloisite25A, PMMA–Cloisite20A, and PMMA–Cloisite30B). The 001 peaks for the systems were observed around angles of  $2\theta = 2.5$ – $3.0^\circ$ , clearly indicating that the intercalation of PMMA into the clay layers had taken place in all of the systems with the organoclays. The  $d$ -spacings are provided in Table I. The comparison of the diffraction patterns for each hybrid with the re-

**TABLE I**  
WAXD  $d$ -Spacings of Various Hybrids Made from Different Organoclays and PMMA Compared with the  $d$ -Spacings of the Organoclays Alone

Organoclay	$d$ -Spacing in (Å)			$\Delta d$ for the first peak
	First peak	Second peak	Third peak	
30B + PMMA	32	16.4	11.4	14.0
30B	18			
20A + PMMA	32.2	17	11.4	7.0
20 A	25.2	12.4		
10A + PMMA	34.04	17.1	11.8	14.2
10 A	19.8			
25 A + PMMA	32.7	16.6	11.1	13.7
25 A	19.0			

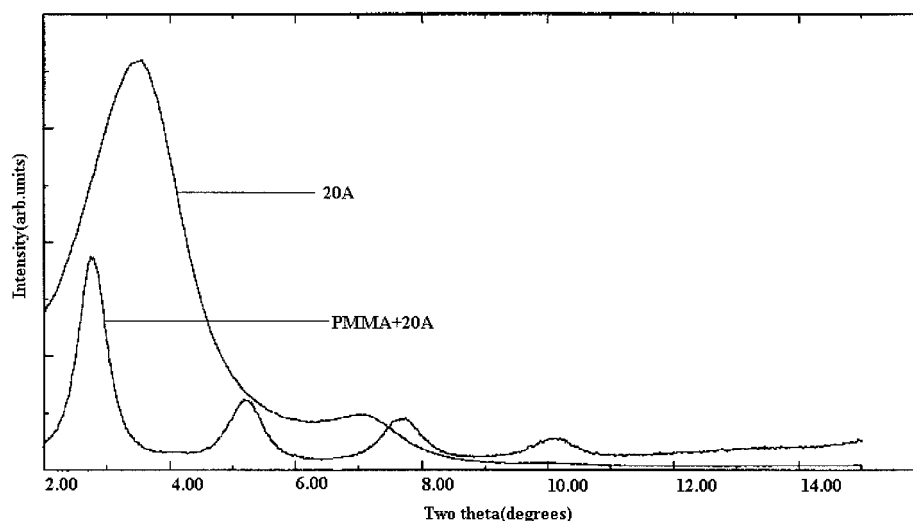


Figure 3 WAXD patterns for Cloisite20A and its nanocomposite with PMMA.

spective organoclay (Cloisite20A, Cloisite25A, Cloisite10A, and Cloisite30B) are presented in Figures 3–6. In the case of the hybrid with NaMT, as seen in Figure 4, there was no intercalation by the polymer, but the peak intensity diminished. Further conjectures on this behavior were not possible at this time with the type of the characterization used in this work, and a direct comparison of WAXD intensities, among nanocomposites and organoclays, could not be used as a measure of the dispersability of clay layer stacks. However, clearly, PMMA could not intercalate into pristine montmorillonite, as shown by our results. On the basis of peak broadening, this also, to a certain extent, may have indicated some level of a reduction in the number of clay platelets per stack in the polymer matrix, resulting from either the processing used to prepare the nanocomposite or a possible nonnanoscopic favorable interaction between NaMT and

PMMA. This may, therefore, have resulted in little dispersion of the clay stacks in the PMMA matrix relative to the tightly stacked and much longer ranged order in the case of NaMT clay.

In all four hybrids with the specific organoclays, there was sufficient intercalation, by way of a change in the  $d$ -spacing of around 14 Å, except in the case of PMMA–Cloisite20-A, where there was an increase of about 7 Å only. The actual (001)  $d$ -spacings for the interlayers containing the polymer were almost the same for all systems (around 33–34 Å). The interlayer  $d$ -spacings for the organoclays were all around 19–20 Å, except for Cloisite20A, where it was 25.2 Å. In the case of the hybrids with Cloisite30B, Cloisite10A, and Cloisite25A, the similar organoclay  $d$ -spacings among the clays and similar  $d$ -spacings among their respective nanohybrids led us to the conclusion that the chemical potential and polymer–clay interactions of

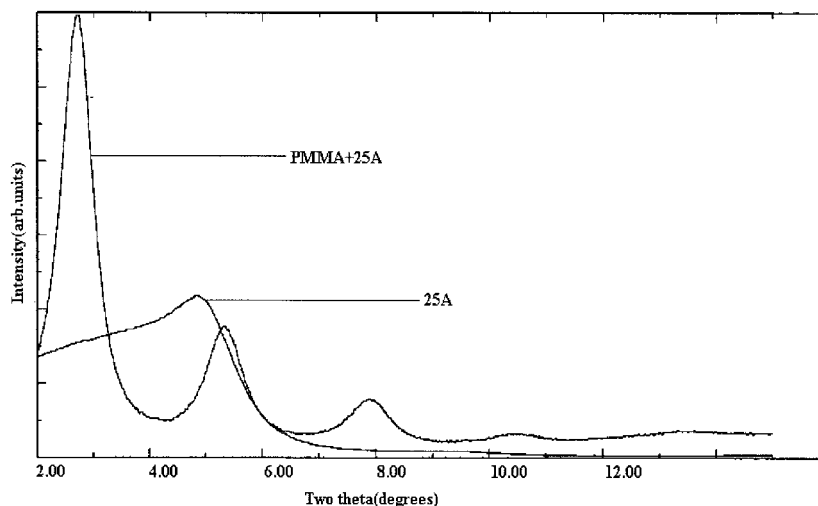


Figure 4 WAXD patterns for Cloisite25A and its nanocomposite with PMMA.

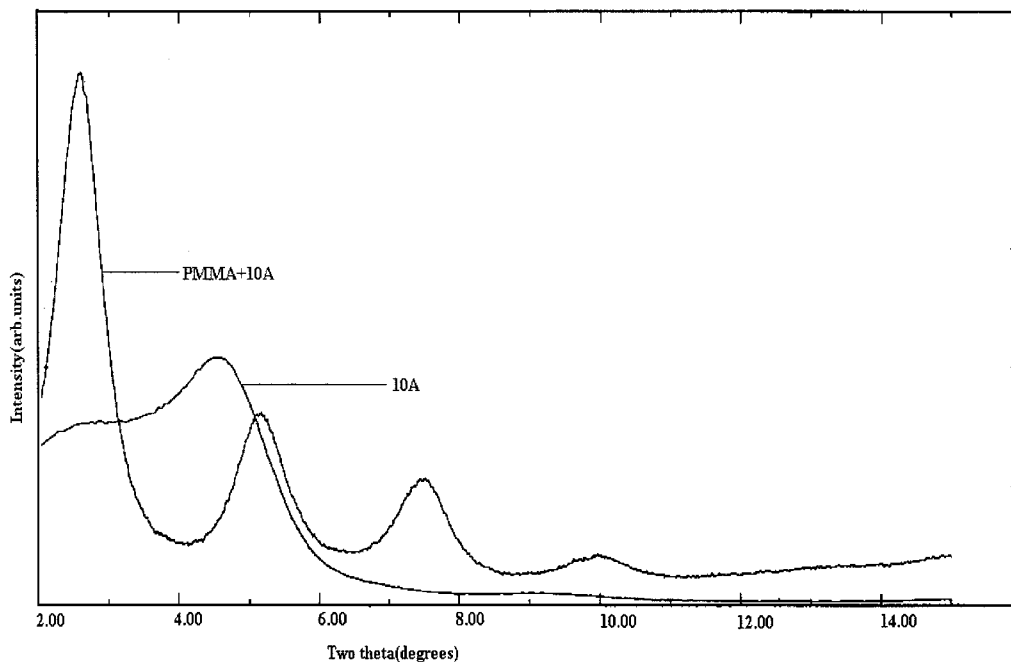


Figure 5 WAXD patterns for Cloisite10A and its nanocomposite with PMMA.

these systems were fairly equal. This was an interesting observation if one considers that the chemical structures of the modifiers were quite different in these organoclays. However, the organic modifier in each of these clays was a single tallow amine (the tallow being a mixture of alkyl chains C18, C16, and C14), and therefore, the single long alkyl chain per amine molecule seemed to be controlling the three-way miscibility interaction between the clay framework, the amine itself, and PMMA segments.

The lower amount of intercalated polymer in the case of the hybrid with Cloisite20A seemed to arise because of a lower extent of favorable interaction and because the ditallow modifier contained a greater

number of hydrophobic  $\text{CH}_2$  groups relative to the other modifiers, which had only a single tallow alkyl chain. A comparison of the grafting densities (equivalently through the CEC) of the organoclays Cloisite20A (CEC = 95 meq/100 g), Cloisite30B (CEC = 90 meq/100 g), Cloisite25A (CEC = 95 meq/100 g), and Cloisite10A (CEC = 125 meq/100 g) clearly indicated that in Cloisite20A, Cloisite25A, and Cloisite30B, the number of organic amine molecules per standard area of clay surface was similar. Therefore, greater the number of  $\text{CH}_2$  groups per amine molecule was, the less favorable was the interaction between the intercalated polymer segments and the clay surfaces as well as the interaction between the polymer segments

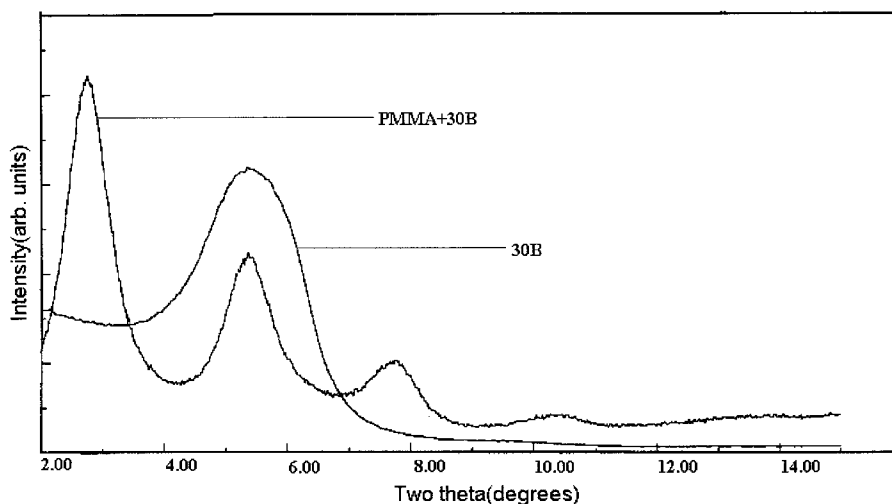


Figure 6 WAXD patterns for Cloisite30B and its nanocomposite with PMMA.

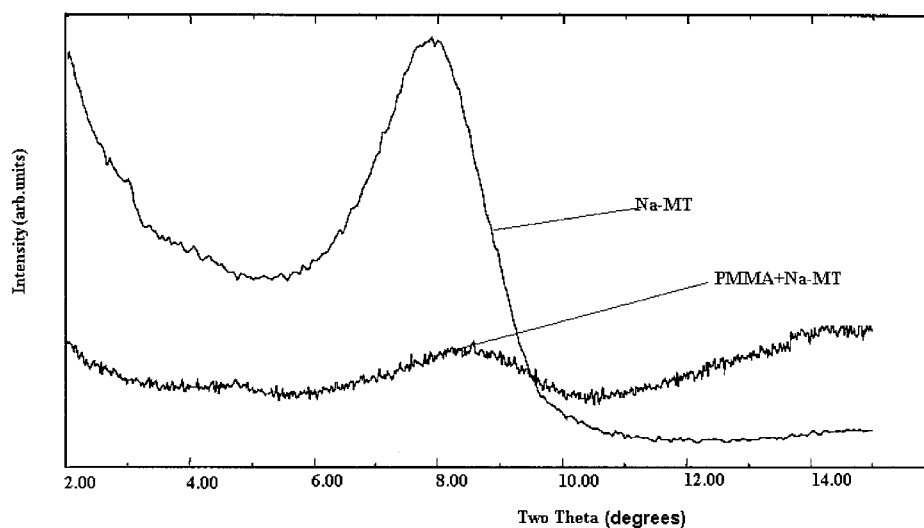


Figure 7 WAXD patterns for Na<sup>+</sup>MT and PMMA nanocomposites prepared with Na<sup>+</sup>MT.

and the organic modifier segments. This rationalization was used to explain the behavior of PMMA-Cloisite20A relative to that of PMMA-Cloisite25A and PMMA-Cloisite30B. In the case of PMMA-Cloisite10A, even though the amine grafting density was higher (125 meq/100 g), the number of CH<sub>2</sub> groups per amine molecule was lower by a factor of 2 (single tallow relative to ditallow), whereas the increase in the grafting density per area of clay surface was not higher by a factor of 2 (125/90 is roughly a factor of 1.4 only). PMMA is relative more polar than an alkyl chain, and so beyond a particular length of the alkyl group on the amine modifier, the miscibility of the clay with PMMA may not have been favored. Experiments with a far lesser number of CH<sub>2</sub> groups per amine molecule would need to be performed in the future to ascertain the minimum number of CH<sub>2</sub> groups required on the amine to promote intercalation and a more comprehensive understanding of the molecular thermodynamics of these systems.

The peaks from XRD studies for all of the intercalated systems were narrow, indicating a high stacking order of the successive clay layers in the hybrid matrix. The strong Bragg diffraction peaks reflected coherent stacking of the clay platelets and, thus, the presence of an ordered structure in the hybrid. However, we observed the higher order reflections of the (001) peak, that is, the (002) and (003) peaks, as present in the hybrids, which indicated that PMMA had diffused inside the interlayer gallery of the clays without significantly disrupting the layer structure of the clays. Also, a broadening of the organoclay peak indicated that the clays had dispersed somewhat in the overall polymer matrix.

From the XRD patterns shown in Figure 2, we concluded that the organoclay Cloisite10A gave the maximum interlayer gallery *d*-spacing. Because the or-

ganoclay gave the largest value of change in *d*-spacing with polymer intercalation, we realized that Cloisite10A provided the most favorable interaction between the polymer and the clay. From the results, it was also apparent that because the organic modifiers themselves and PMMA were essentially incompatible, leading to a preference of the modifier chains to lie close to the silicate surface (albeit with a loss in entropy), a certain amount of exposed silicate surface was required for the PMMA to interact favorably with the silicate, as the results for the ditallow versus the single tallow modified systems indicated. However, the complete exposure of the silicate surface was an unfavorable situation for the polymer. The TEM micrographs for the PMMA-Cloisite25A nanocomposite, as a sample of the structure of the organoclay-based intercalated PMMA nanocomposites prepared by melt processing, are provided in Figure 8. Individual intercalation layers are shown clearly in Figure 8(b), at high magnification, whereas the overall phase clearly showed the clay layer stacks dispersed in the PMMA matrix, as shown in Figure 8(a).

### Thermal properties of the hybrids

The TGA results on PMMA and its nanocomposites, as shown in Figure 9, revealed that the onset temperature of thermal decomposition went up by a magnitude of around 15–30°C, as measured at 5% decomposition, by the addition of clays to the polymer matrix. This thermal behavior was caused by the insertion of PMMA between the layers of montmorillonite, which provided resistance to the thermal degradation of PMMA. The decomposition temperatures at 5% weight loss are provided in Table II. As was evident, the onset of decomposition for the PMMA-NaMT hybrid was greater by 15°C compared to that of PMMA,

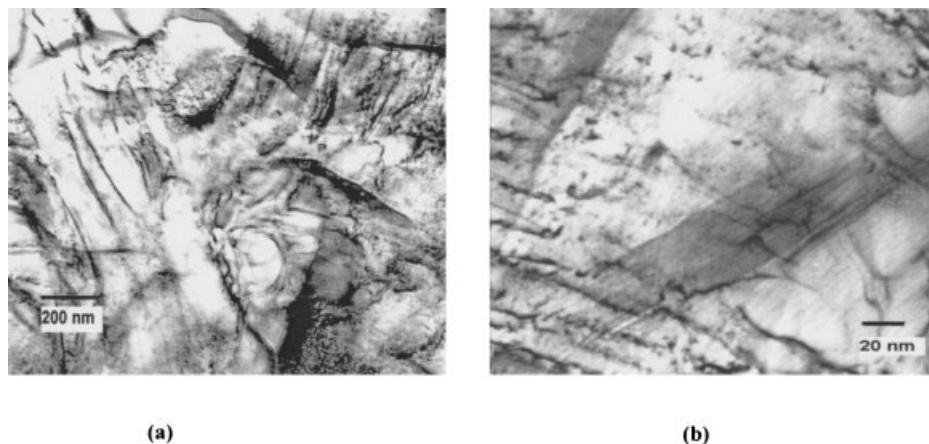


**Figure 8** TEM micrographs of the PMMA–Cloisite25A nanocomposite taken with ultramicrotomed sections: (a) low magnification (40,000 $\times$ ), showing clay stacks dispersed in the PMMA matrix, and (b) high magnification (250,000 $\times$ ), showing individual clay layers in a clay stack.

indicating a significant improvement in the ability of the hybrid to withstand degradation. Improvement in the thermal stability of a PMMA nanocomposite was also reported earlier by Blumstein,<sup>14</sup> however, the 5%-weight-loss temperature was around 265 $^{\circ}\text{C}$ , which is lower than the temperature observed for PMMA–NaMT hybrids in this study. The final loss temperature, where the polymer degraded completely (around slightly greater than 90% degradation in the case of the hybrid, inclusive of the organic amine, and 100% degradation in the case of the unfilled polymer) was almost the same when PMMA was compared with its hybrid with NaMT clay. This indicated that the thermal insulation effect that occurs because of the shielding of the intercalated polymer chains by the confining clay layers did not occur in the case of the PMMA–NaMT hybrid. This was also shown to be the case earlier by the XRD results, where no intercalation was evident in the case of the PMMA–NaMT hybrid. The onset of decomposition in the case of the hybrids with the four organoclays, however, increased much more

in the case of the systems prepared with Cloisite20A and Cloisite25A. These were also the systems that had a relatively larger amount of intercalated polymer compared to the other systems. Even though the extent of intercalation in PMMA was greatest in the case of the most polar organoclay, Cloisite30B, facilitating the largest level of favorable miscibility with the polymer, the degradation improvement in this case was not the best among these systems. One of the possible reasons could have been the higher thermal stability of the organic modifiers in the case of Cloisite25A (a single tallow modifier with a ethylhexyl group, which showed an onset of 358 $^{\circ}\text{C}$ ) and Cloisite20A (a ditallow modifier, which showed an onset of 363 $^{\circ}\text{C}$ ) compared to Cloisite30B (a single tallow modifier with two ethanol groups).

We compared our results with those provided in a recent report of Hwu et al.<sup>15</sup> In their study also, the incorporation of clay layers into the PMMA matrix resulted in an enhancement of the thermal stability of the nanocomposites (by about 40 $^{\circ}\text{C}$  for the main-chain degradation of PMMA, from 329 $^{\circ}\text{C}$  for virgin PMMA to about 370 $^{\circ}\text{C}$  for the nanocomposite). In our case, as shown in Table II, the enhancement was from 331 $^{\circ}\text{C}$  (for unfilled PMMA) to 363 $^{\circ}\text{C}$  for the best organoclay nanocomposite candidate.

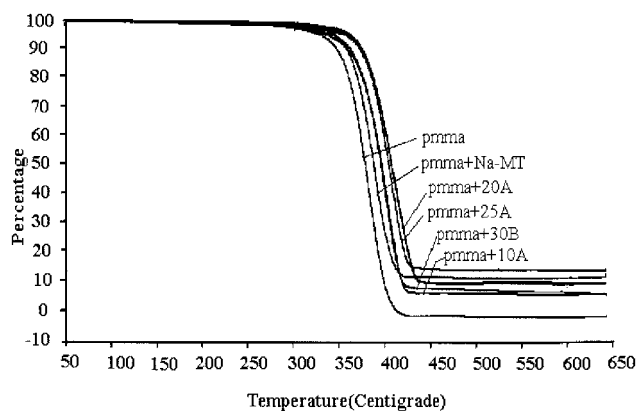


**Figure 9** TGA thermographs of PMMA and the nanocomposites with the organoclays.

**TABLE II**  
Onset of Thermal Decomposition (5%) of PMMA and Its Various Hybrids at 10% Clay Loading

System	Onset of thermal decomposition ( $^{\circ}\text{C}$ )
PMMA	331.26
PMMA/CloisiteNaMMT	346.2
PMMA/Cloisite10A	343.9
PMMA/Cloisite20A	362.72
PMMA/Cloisite25A	357.75
PMMA/Cloisite30B	338.31

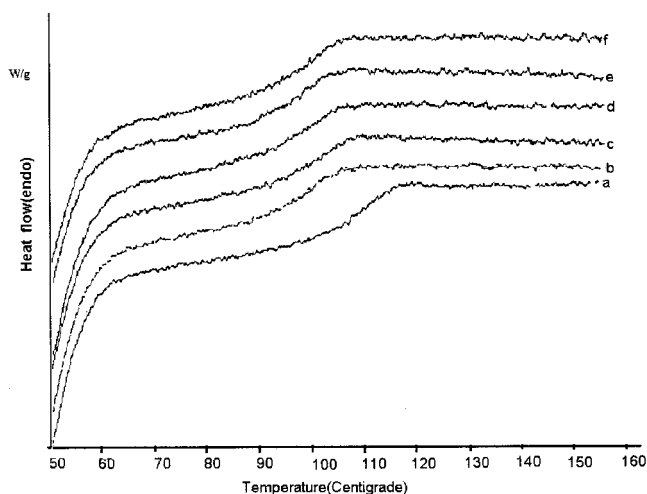


**Figure 10** DSC thermographs of PMMA and its nanocomposites with the organoclays: (a) PMMA, (b) PMMA-Cloisite20A, (c) PMMA-Cloisite30B, (d) PMMA-Cloisite10A, (e) PMMA-NaMT, and (f) PMMA-Cloisite25A.

The effect of intercalation and the confinement of polymer by the clay layers on the  $T_g$  and thermal response was also studied with dynamic DSC. The DSC thermographs are shown in Figure 10. DSC isotherms of PMMA and the nanocomposites showed evidence of a second-order transition ( $T_g$ ); however, there was no first-order transition, showing the absence of melting temperature, which was caused by the amorphous nature of the polymer. As shown in Table III, the  $T_g$  of the nanocomposites decreased by a magnitude of 10–12°C (~10%) relative to PMMA. The  $T_g$  of PMMA obtained here (108.6°C) compared well with the value reported for atactic PMMA (105°C but with an average molecular weight; the melt flow index was not provided).<sup>16</sup> The  $T_g$  of all the hybrids with the organoclays used in this study were roughly the same (within 1–2°C), whereas there was a larger drop in the  $T_g$  in the case of the hybrid with NaMT.

The reason for the differences in reduction in the  $T_g$  between the hybrids formed with unmodified MMT and organically modified MMT is not very clear at this time because a reduction in  $T_g$  due to the enhanced mobility of confined chains in a intercalated system, as shown here by the hybrids with the organoclays, should lead to a situation where the unintercalated hybrid formed by unmodified NaMT gave a smaller reduction in  $T_g$  compared to the hybrids formed with modified clays. The existence of a thin interface layer, which is more mobile for neutral or weakly attractive surfaces, or thin polymer layers in two-dimensional confinement as in the interlayer gallery tends to lower the  $T_g$  and enhance the segmental dynamics of the polymer chains and, therefore, some part of the overall hybrid.<sup>17</sup> The depression in surface  $T_g$  or confined-film  $T_g$  of the polymer may have also partly been due to reduction in density caused by chain-end localiza-

tion and loss in entanglements as compared to the bulk matrix; however, this situation exists in all intercalated polymer systems (even where an increase in the  $T_g$  is experimentally found). Therefore, a decrease in  $T_g$  due to intercalated hybrid formation is very much a polymer-system-dependent behavior and also depends on the specific interactions between polymer segments, the organoclay modifier, and the clay surface and layer atoms. The decrease in  $T_g$  in our study is in agreement with the results of Giannelis and colleagues<sup>11,12</sup> by the melt intercalation route of PMMA nanocomposite preparation. Further investigations to understand the molecular events underlying the lowering of  $T_g$  are currently ongoing in our laboratory. We also studied the mechanical and dynamic mechanical properties of these hybrids, and the observations between the DMA results and the DSC results presented here will be reported in another article.

Very recently, Hwu et al.<sup>15</sup> reported studies on PMMA nanocomposites prepared with stearyltrimethyl-ammonium-modified montmorillonites. Their base montmorillonite was the same in terms of the source and the CEC as in this study. The samples in that study were prepared with a solution-mixing route. Their thermal study showed a significant enhancement in the  $T_g$  of the nanocomposite ( $T_g = 124^\circ\text{C}$ ) compared to unfilled PMMA. The  $d_{001}$  spacings for the nanocomposite were not provided in that article; however, TEM micrographs showed a dispersion of clay stacks in the PMMA matrix. Also, the molecular weights of PMMA used in their work were lower than those used in this study; therefore, the  $T_g$  that they reported for unfilled PMMA was 82°C and was lower compared to the  $T_g$  we report, which was 108°C (for high-molecular-weight PMMA). Therefore, a direct comparison of the  $T_g$  values between the results of Hwu et al. and this study for the nanocomposites could not be made. The  $T_g$  of intercalated polymer nanocomposites is a complicated function of the nature of the organic modifier, weight loading of clay, the mean dominant  $d_{001}$  spacings of the interlayer gallery space, and the dispersion and arrangement of the clay stacks in the polymer matrix.

The dynamics of polymer segments, which control the overall  $T_g$ , depend on the previously mentioned

**TABLE III**  
 $T_g$ 's of PMMA and Various Hybrids at  
10% Clay Loading

System	$T_g$ (°C)
PMMA	108.6
PMMA/NaMMT	97
PMMA/Cloisite10A	98.7
PMMA/Cloisite20A	99.1
PMMA/Cloisite25A	98.8
PMMA/Cloisite30B	100



factors in the following way, as is known from previous results on polymer–clay systems and the rationalization of the polymer dynamics in the condensed phase:

1. The dynamics of confined chains between successive clay layers can either be faster or slower than in the bulk phase, depending on the specific physical chemistry interactions between the segments and the clay layer atoms, which are controlled essentially by the type of organic modifier when the base montmorillonite is unchanged.
2. The dynamics of the segments between clay stacks is dictated by the average interstack distances in the matrix, which is determined by the extent of dispersion of the clay stacks in the matrix. This effect depends on the overall thermodynamic interaction and the processing conditions used to prepare the nanocomposite.
3. The overall dynamics are affected by and contributed by the average interstack distances and the interlayer *d*-spacings, which are dictated by the weight loading of the clay into the polymer matrix.

Other factors, such as the lateral dimensions of the clay platelets, also affect the dispersability of the clay and control the spatial distance distributions between clay stacks in the polymer matrix. Because of these considerations, controlled studies in future that can suitably discern the independent role of these factors would be necessary to understand the molecular structure–glass-transition property aspects of such complex systems. We also performed studies involving variation of the processing conditions (to be reported in a future publication), whereby the  $T_g$ 's were found to improve for the nanocomposite compared to unfilled polymer. However, this effect was dependent on the organoclay used for the nanocomposite preparation, as in some cases (with specific types of organoclays), it was found that the  $T_g$ 's were truly lower for the nanocomposite than for the virgin polymer, even though the *d*-spacings were different on the basis of the processing conditions.

## CONCLUSIONS

PMMA clay nanocomposites were prepared by a simple melt mixing method, and a study was performed to investigate the effect of various types of organoclays on the formation of intercalated PMMA nanohybrids. WAXD results for the hybrids prepared with unmodified NaMT and various organically modified MMTs showed that presence of an organic modifier

was necessary for the intercalation of PMMA into montmorillonite at the CEC that was used. Hybrids prepared with a single tallow modifier with varying degrees of hydrophobicity all showed a separation of the clay layers on the order of 7–14 Å, with the relatively more polar organoclays showing greater extents of intercalation. A single tallow amine appeared to control the polymer–clay miscibility more favorably than a ditallow amine among the modifiers we used. The degradation onset temperature increased by 15–30°C, indicating improved thermal stability of the nanocomposites. The improvement in thermal stability was more pronounced in the case of hybrids formed by Cloisite20A and Cloisite25A relative to Cloisite30B and Cloisite10A because of the greater thermal stability of the former organoclays and the formed nanostructures arising from their chemical structure. The  $T_g$  of the nanocomposites decreased by a magnitude of 10–12°C (~10%) relative to that of PMMA. The driving force for the reduction in the  $T_g$  due to hybrid formation and the relative differences in the reduction among the various hybrids were not apparent; however, other types of experimental investigations are required to ascertain the molecular mechanisms responsible for such behavior.

We thank the Council of Scientific and Industrial Research, India, for providing S.K. with a Graduate Junior Research Fellowship. We are also thankful and appreciate the generous gift of the clay samples by Southern Clay Products, Inc.

## References

1. Giannelis, E. P.; Krishnamoorti, R.; Manias, E. *Adv Polym Sci* 1999, 138, 107.
2. Giannelis, E. P. *Adv Mater* 1996, 8, 29.
3. Lagaly, G. *Appl Clay Sci* 1999, 15, 1.
4. Gilman, J. *Appl Clay Sci* 1999, 15, 31.
5. Blumstein, A. *J Polym Sci Part A: Gen Pap* 1965, 3, 2653.
6. Biasci, L.; Aglietto, M.; Ruggeri, G.; Ciardelli, F. *Polymer* 1994, 35, 3296.
7. Lee, D. C.; Jang, L. W. *J Appl Polym Sci* 1996, 61, 1117.
8. Chen, G.; Chen, X.; Lin, Z.; Ye, W. *J Mater Sci Lett* 1999, 18, 1761.
9. Okamoto, M.; Morita, S.; Taguchi, H.; Kim, Y. H.; Kotaka, T.; Tateyama, H. *Polymer* 2000, 41, 3887.
10. Huang, X.; Brittain, W. J. *Macromolecules* 2001, 34, 3255.
11. Bandyopadhyay, S.; Giannelis, E. P.; Hsieh, A. J. *Polym Prepr* 2000, 82, 208.
12. Hsieh, A. J.; Giannelis, E. P. Presented at the American Physical Society Symposia Presentation, Atlanta, GA, March 1999.
13. Salahuddin, N.; Shehata, M. *Polymer* 2001, 42, 8379.
14. Blumstein, A. *J Polym Sci Part A: Gen Pap* 1965, 3, 2665.
15. Hwu, J. M.; Jiang, G. J.; Gao, Z. M.; Xie, W.; Pan, W. P. *J Appl Polym Sci* 2002, 83, 1702.
16. Brandrup, J.; Immergut, E. H. *Polymer Handbook*, 3rd ed.; Wiley Interscience: New York, 1989.
17. Anastasiadis, S. H.; Karatasos, K.; Vlachos, G.; Manias, E.; Giannelis, E. P. *Phys Rev Lett* 2000, 84, 915.